LANGMUIR

pubs.acs.org/Langmuir Article

Control of Vancomycin Activity through the Encapsulation and Controlled Release from a Propargyl Acrylate−Poloxamer Nanocomposite System

Oleksandr Klep, Haley W. Jones, Vladimir Reukov, and Stephen H. Foulger*

Cite This: *Langmuir* 2020, 36, 14607−14613 Read Online

ACCESS | Metrics & More | Article Recommendations

ABSTRACT: Vancomycin is a potent antibacterial drug that suffers from poor bioavailability due to its poor water solubility and relatively high molecular weight. Consequently, the application of vancomycin to treat bacteria-induced disease is limited. In this study, the ability of a temperature-stimulated propargyl acrylate−poloxamer nanocomposite (PAPN) system to encapsulate and release vancomycin is investigated. A controllable encapsulation and release system can be used to not only increase and prolong the bioavailability of vancomycin but also activate vancomycin with a temperature change. The PAPN system was prepared using an emulsion polymerization of propargyl acrylate followed by a surface decoration with a poloxamer at a precisely controlled grafting density. The activity of the PAPN system loaded with vancomycin is compared to that of the free drug and unmodified propargyl acrylate nanoparticles. It is shown that the activity of the PAPN system loaded with vancomycin is comparable to that of a freshly prepared, free-floating vancomycin solution. Upon storage, the activity of the free vancomycin in solution decreases, while the PAPN system loaded with vancomycin retains its high activity. Additionally, the PAPN system is able to effectively encapsulate and deactivate vancomycin until heated above a lower critical solution temperature (LCST). At temperatures above the LCST, the PAPN system releases vancomycin restoring the activity of the drug.

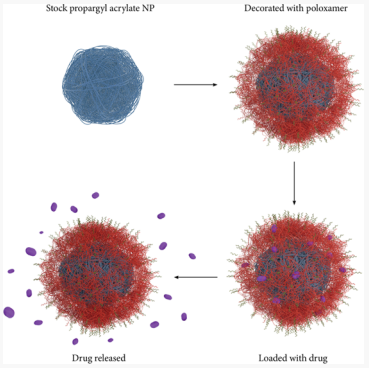

INTRODUCTION

Controlled release of biologically active molecules is superior to a simple injection of free, active molecules in solution because it allows for a regulated concentration of the active molecule throughout the body. This regulation limits the side effects of the active molecules and increases treatment efficiency.[1−4] Additionally, controlled release allows for a high concentration of active molecules to be located at a site of interest while simultaneously maintaining a safe level of the active molecules at other organs and systems in the body.[5,6] One of the mechanisms used to achieve controlled drug delivery is the absorption−resorption of the drug into an active layer on a carrier.[7−9] The drug vancomycin is an ideal candidate for a controlled drug delivery system due to its high activity toward a multitude of bacteria strains but limited stability in aqueous solutions.[10−13] Various systems that are able to encapsulate and release vancomycin have been developed;[7,14−17] however, many of these approaches suffer from one of two common pitfalls. The first of which arises from complex synthesis mechanisms, which result in a costly final price. The second includes a lack of control over the release patterns of the system placing strict limitations on its application conditions, which make it useful for a narrow range of patients.

Described here is a drug delivery device composed of a biocompatible propargyl acrylate (PA) nanoparticle modified with a poloxamer block copolymer to achieve a temperature-triggered drug release. A PA core has shown to provide a versatile platform for medical applications.[18−20] Alkyne groups that decorate the surface of a PA nanoparticle serve as anchoring points that can be used to attach various active molecules through a copper(I)-catalyzed azide/alkyne cycloaddition (CuAAC) click reaction. Click reactions offer the ability to covalently connect two molecules under mild conditions and with very high selectivity.[21,22] Click reactions are of particular interest when working with biologically active molecules due to the preserved biological activity of the molecules in the mild reaction conditions.

In recent years, the group of triblock copolymers known as poloxamers have been investigated for their use in medical applications. Poloxamers possess temperature-responsive behavior and are able to stabilize various active molecules in

Received: August 13, 2020
Revised: October 19, 2020
Published: November 24, 2020

https://dx.doi.org/10.1021/acs.langmuir.0c02385
Langmuir 2020, 36, 14607−14613

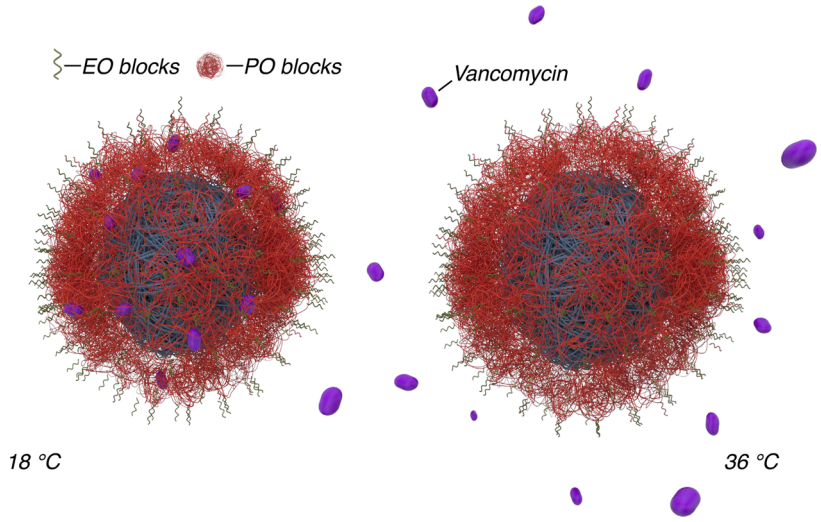

Figure 1. Left image: a PAPN particle below the LCST of the poloxamer, and the shell is expanded such that it can encapsulate vancomycin. Right image: a PAPN particle above the LCST of the poloxamer, and the shell is collapsed such that vancomycin is expelled from the shell and released into the environment. This expulsion results in the drug being reactivated.

aqueous environments.[23,24] Poloxamers are known to form pockets that can hold biologically active molecules with the dimension of these pockets being temperature-dependent.[25,26] This characteristic response allows for the fabrication of a temperature-triggered drug release device where the ability to control the temperature of the drug release is achieved through the selection and ratio of blocks in the poloxamer copolymer.[27,28] This tunable, temperature-triggered release presents an opportunity to use the inherent elevated temperature at a source of inflammation as the trigger for the drug release mechanism. Decoration of a PA core with a poloxamer to form a propargyl acrylate−poloxamer nanocomposite (PAPN) system (Figure 1) creates an active layer on the surface of the PA nanoparticle that can encapsulate vancomycin at temperatures below a lower critical solution temperature (LCST). Upon exposure to a temperature above the LCST, the poloxamer corona collapses triggering the release of the drug. An additional benefit of using a polymer carrier to encapsulate vancomycin is its potential to increase the shelf life of ready-to-use solutions. It has been demonstrated that the encapsulation of vancomycin in a triblock copolymer can protect the drug from the environment and preserve the bioactivity of the drug for extended periods of time when compared to that of pure vancomycin solutions.[29]

EXPERIMENTAL SECTION

Materials and Reagents. All reagents were purchased from Sigma-Aldrich with at least 97% purity level. Solvents were purified using standard procedures.

Characterization. ^{1}H spectra were recorded on JEOL ECX-300 spectrometers (300 MHz for proton). Chemical shifts for protons are reported in parts per million downfield from tetramethylsilane and are referenced to the carbon resonances of the solvent ($CDCl_3$: δ 7.26 or dimethyl sulfoxide (DMSO)-d_6: δ 2.50). Fourier transform infrared (FTIR) spectra were obtained with a Nicolet 6700 Thermo Scientific FTIR spectrometer, and all spectra were measured with FTIR-ATR with a diamond head. Nanoparticle size was checked using a Coulter N4Plus DLS using 10 mm quartz cuvettes. UV spectra were obtained using a Perkin Elmer Lambda 850 spectrometer. Scanning electron microscopy (SEM) was performed on a Hitachi S4800 field emission SEM (FESEM) at a maximum accelerating voltage of 10.0 kV. Images were analyzed using Quartz PCI v.8.5 software package.

Nanoparticle Preparation. Propargyl acrylate (PA) nanoparticles were prepared by an emulsion polymerization in a single-necked round-bottom flask (150 mL) equipped with a magnetic stir bar. Deionized (DI) water (50 mL) was added to the flask and purged with nitrogen for 30 min. Potassium persulfate (60 mg) and an aqueous solution of sodium dodecyl sulfate (70 mg, 29 %) were added to the flask under nitrogen and purged for 5 min. A degassed solution of propargyl acrylate (3 mL) and divinylbenzene (0.45 mL) was added to the flask, purged with nitrogen for 1 min, and the flask was transferred to a preheated bath at 70 °C. The mixture was stirred at 70 °C under nitrogen for 2.5 h with constant stirring. After 2.5 h, the emulsion was allowed to cool and was purified by dialysis. Dialysis was performed using a Spectra/Por Dialysis membrane with MWCO 50000 for 5 days at 30 °C with water changed every 8 h. The resulting PA nanoparticles were characterized using DLS, which gave a median size of 26 ± 6 nm. The concentration of the obtained nanoparticles in water was 50 mg/mL.

Poloxamer Modification. *$MeSO_2$-Pluronic-L62*. Pluronic-L62 (3.14 g, 1.086 mmol) was dissolved in dry dichloromethane (DCM) (10 mL) followed by the addition of triethylamine (0.132 g, 1.3 mmol). The obtained solution was stirred at room temperature, and methanesulfonyl chloride (62 mg, 0.543 mmol) was added dropwise. The mixture was stirred for 6 h at room temperature and then was washed with water. The organic layer was separated, dried with Na_2SO_4, filtered, and evaporated under reduced pressure. The yield was 3.1 g (95%) of a clear oil. This product was used in the following step without further purification. ^{1}H NMR ($CDCl_3$) δ 1.11 (m, 87H), 3.06 (s, 3H), 3.38 (m, 31H), 3.52 (m, 54H), 3.63 (m, 96H), 3.74 (m, 4H), 4.35 (m, 2H)

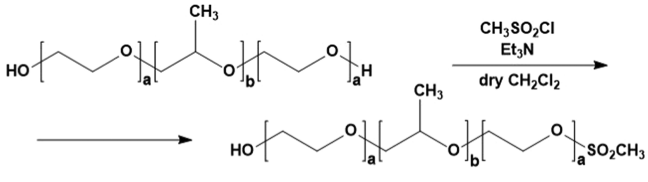

***Pluronic-L62-N_3*.** Sodium azide (195 mg, 3 mmol) was added to a solution of $MeSO_2$-pluronic-L62 (3.1 g, 1.03 mmol) in dimethylformamide (DMF) (10 mL). The mixture was stirred and heated to 80 °C for 3 h. After cooling, the mixture was extracted with DCM and washed twice with water. The organic layer was separated, dried with Na_2SO_4, filtered, and evaporated under reduced pressure. The yield was 2.27 g (75%) of a clear oil. Pluronic-L64-N3 was used in the

https://dx.doi.org/10.1021/acs.langmuir.0c02385
Langmuir 2020, 36, 14607−14613

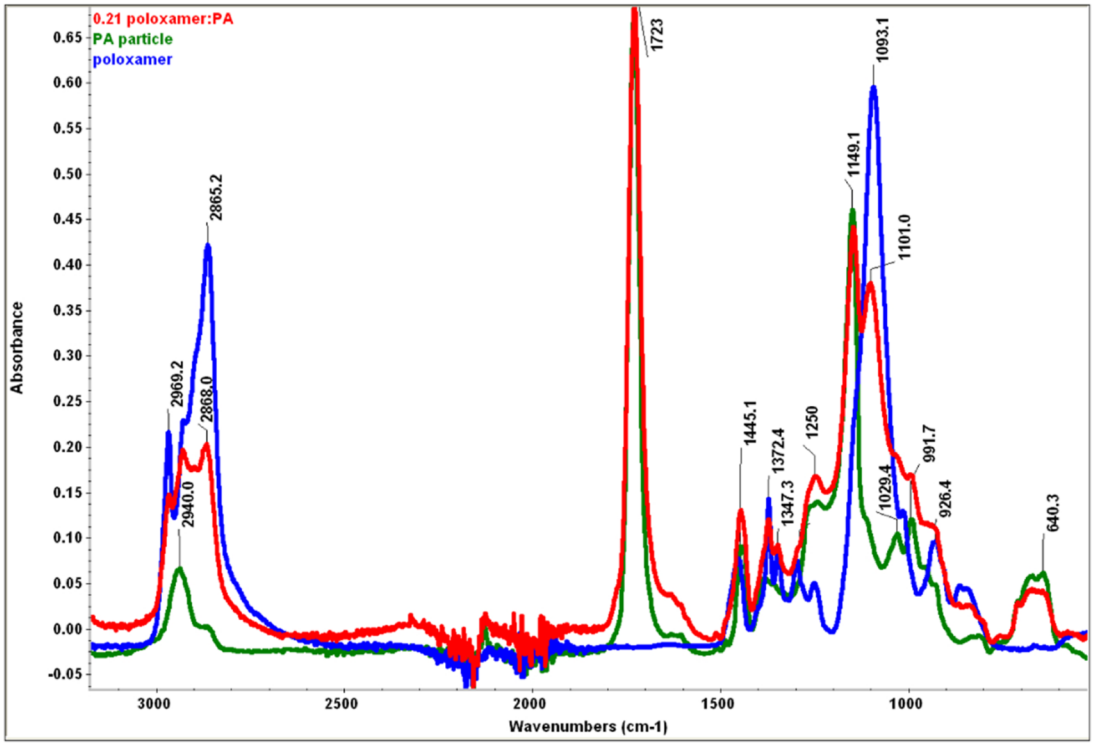

Figure 2. FTIR spectra of PA nanoparticles (green), poloxamer (blue), and PAPN nanoparticles with a known poloxamer content (red) showing good separation of the peaks for poloxamer (1100 cm^{-1}) and PA particles (1150 cm^{-1}). The grafting density of poloxamer in PAPN can be distinguished through the ratio of these two peaks.

following step without further purification. ^1H NMR ($CDCl_3$) δ 1.07 (m, 87H), 3.34 (m, 31H), 3.48 (m, 54H), 3.59 (m, 96H)

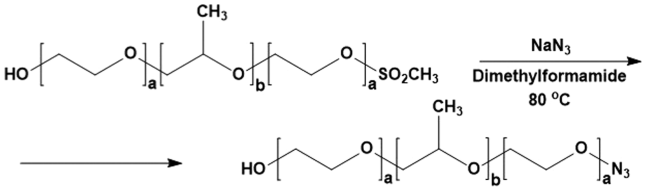

.

Nanoparticle Modification. Nanoparticle modification was performed using a copper(I)-catalyzed azide/alkyne cycloaddition (CuAAC) click reaction. The general click reaction procedure was used as described elsewhere[10]. In short, a solution of pluronic-L62-N_3 (0.1 g, 0.05 mmol) in methanol (20 mL) was added to a solution of copper(II) sulfate (10 mg, 0.04 mmol) dissolved in 5 mL of DI-H_2O. After 5 min, a solution of PA nanoparticles (5 mL of a 50 mg/mL solution) was added to the reaction. The reaction was stirred and purged with nitrogen for 5 min followed by the addition of sodium ascorbate (40 mg, 0.2 mmol). The reaction continued at 25 °C for 3 h under nitrogen. The resulting reaction mixture was centrifuged at 7000*g* for 25 min. The separated nanoparticles were washed with a mixture of DI-H_2O/methanol 1:1 (40 mL) until the poloxamer content in the precipitate became constant as measured by FTIR.

Molar Extinction Coefficient of Vancomycin. Molar extinction of vancomycin was calculated in DI water to be 6.53 M/cm at 280 nm using multiple solutions of concentrations 0.5, 0.25, 0.125, and 0.0625 mg/mL.

Bacterial Analysis. Ward's live *Escherichia coli* bacterial cultures were obtained from VWR (470176-528), and methicillin-resistant *Staphylococcus aureus* bacterial cultures were obtained from ATCC (33591).

RESULTS

Characterization of PAPN. The grafting density of poloxamer on the propargyl acrylate (PA) core was determined using Fourier transform infrared spectroscopy (FTIR). FTIR spectra were collected on a set of samples with known ratios of poloxamer to PA. Poloxamer has a strong peak around 1100 cm^{-1}, and PA has a strong peak at 1150 cm^{-1}. Based on the ratios of these two peaks in the FTIR spectra of the poloxamer−PA samples, a calibration curve was obtained. Using this calibration curve, the poloxamer content in the propargyl acrylate−poloxamer nanocomposite (PAPN) system was determined. Figure 2 shows the FTIR spectra of unmodified PA nanoparticles, poloxamer, and PAPN nanoparticles with a poloxamer content of 21 mass %. An experimental precision of less than 1 mass % of poloxamer in the mixture was confirmed.

To convert the mass ratio of poloxamer in PAPN to a grafting density, the size of the PA cores is required. Data from two techniques was combined to determine the size and size distribution of the PA cores in PAPN particles. Scanning electron microscopy (SEM) provided visual confirmation for the shape, size, and size distribution of the PA nanoparticles before and after poloxamer attachment. These results were compared to that of dynamic light scattering (DLS). DLS measurements require a stable sample suspension, and reliable measurements can only be achieved if the nanoparticles have a solid shell that scatters light in a predictable pattern. PAPN particles have a soft, fluid-like shell of poloxamer chains that cause unpredictable light scattering, which results in false DLS readouts. DLS measurements of the PAPN particles were inconsistent at all temperatures and concentrations; therefore, core size determination was based only on the SEM results. For each sample observed with SEM, 200 cores were

https://dx.doi.org/10.1021/acs.langmuir.0c02385
Langmuir 2020, 36, 14607−14613

measured. The average size of the unmodified PA nanoparticles was 26.9 ± 2.84 nm, and the average size of the poloxamer-modified PAPN particles was 29 ± 6 nm. Figure 3 shows SEM images of the unmodified PA nanoparticles and the modified PAPN nanoparticles.

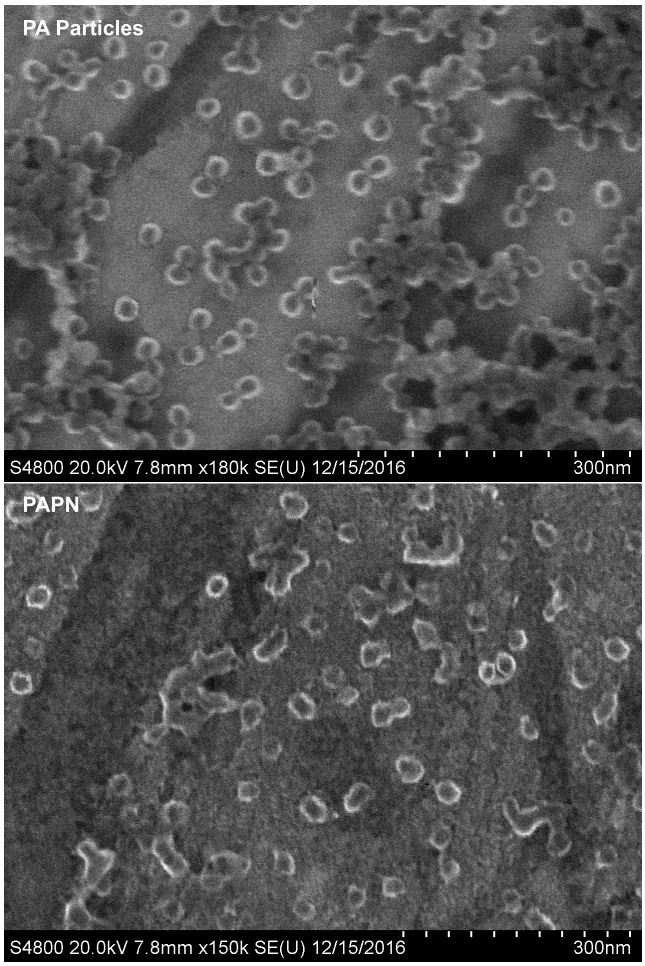

Figure 3. Top image: SEM image of unmodified PA nanoparticles showing good size distribution and regular shapes. Bottom image: SEM image of PAPN nanoparticles showing an increase in not only size and size distribution but also a change in shape from regular spheres to irregular geometries. This shape change can be attributed to the soft nature of the shell.

Based on the PA core size, the grafting density of the poloxamer on the particles was determined to be 0.29 poloxamer chains per nm^2 of the PA core surface. This grafting density was experimentally confirmed to be optimal for small-molecule encapsulation and temperature-triggered release from the PAPN particles. Figure 1 demonstrates the proposed positioning of the vancomycin molecules inside of the poloxamer shell of the PAPN system. Higher grafting densities of the poloxamer lead to a decrease in its encapsulation capacity. This decrease in encapsulation capacity can be attributed to the volume of the poloxamer shell that was accessible for small molecules at lower grafting densities being occupied by poloxamer chains. At lower grafting densities, areas of the PAPN particle core remain exposed allowing small molecules to be adsorbed directly onto the core rather than become trapped in the poloxamer shell. This adsorption inhibits the temperature-triggered release of the small molecules rendering the PAPN system ineffective for the intended use. At low grafting densities, PAPN particles perform as a "grab-only" system rather than a "grab-and-release" system.

Binding Yield of Vancomycin. The encapsulation capacity of the poloxamer shell on the PAPN particles was achieved at approximately 0.5 vancomycin molecules per nm^2 of the PAPN surface. To assess the encapsulation efficiency of the poloxamer shell, excess vancomycin was added to a suspension of PAPN particles held at a temperature below the LCST of the poloxamer. The LCST of the poloxamer used in this study was 18 °C. The mixture was held at this temperature for 24 h to allow enough time for the vancomycin molecules to penetrate the poloxamer shell and reach an equilibrium state. After 24 h, the mixture was centrifuged at 6000 *g* and 7 °C for 40 min. The vancomycin content in the supernatant was calculated based on the molar extinction coefficient of vancomycin in DI-H_2O and the volume of the supernatant collected. Unmodified PA particles encapsulated 0.319 mg of vancomycin per mg of dry cores or 0.76 vancomycin molecules per nm^2 of the core surface. The PAPN system encapsulated 0.189 mg of vancomycin per mg of dry cores or 0.45 vancomycin molecules per nm^2 of the core surface.

Antibacterial Activity. The efficiency of the temperature-triggered release of vancomycin from the PAPN nanoparticles was compared to that of the unmodified PA nanoparticles and the free drug. PAPN nanoparticles without the drug were used as a control for the PAPN particle toxicity. The efficiency of the PAPN system was tested on *E. coli* and *S. aureus* bacteria. The bacterial cultures were incubated in fresh media for 24 h and diluted 5×10^6 times prior to being exposed to PAPN particles and various control samples. An equivalent of 1.4 mg PA cores of each sample was added to 5 mL of bacteria in a phosphate-buffered saline (PBS) solution. In the vancomycin-only sample, 0.25 mg of vancomycin was added, which is comparable to the amount of vancomycin added with the PAPN sample. Samples were incubated for 24 h at both 18 and 36 °C. After incubation, the number of surviving colonies was determined using a colony forming unit (CFU) counting method where 0.1 mL of each sample was seeded on a trypticase soy agar-coated Petri dish with growing media and the bacteria were incubated overnight in a water-jacketed CO_2 incubator at 37 °C. Each sample was prepared in triplicates. The bacterial viability was determined by counting the number of colonies per Petri dish for each sample and comparing it to the number of colonies in the respective control sample. The results are shown in Figure 4 as percentages compared to each control (ex: the surviving *E. coli* colonies incubated with various samples at 18 °C are normalized to the *E. coli* control at 18 °C and are plotted as a percentage).

E. coli bacterial cultures were treated with samples that were stored in water solutions for 2 weeks, while the *S. aureus* bacterial cultures were treated with freshly prepared solutions and solutions that were stored at room temperature for 1 month. Unmodified PA nanoparticles with adsorbed vancomycin (0GD + vanc) had some effect on both bacterial cultures with an inconclusive temperature dependence. These results were expected due to the lack of temperature-dependent components on the unmodified PA nanoparticles; however, any vancomycin that was adsorbed by the PA nanoparticles was held mostly by the hydrophobic interactions, which are temperature- and concentration-dependent. The difference in growth rates of the *E. coli* and *S. aureus* bacterial

https://dx.doi.org/10.1021/acs.langmuir.0c02385
Langmuir 2020, 36, 14607−14613

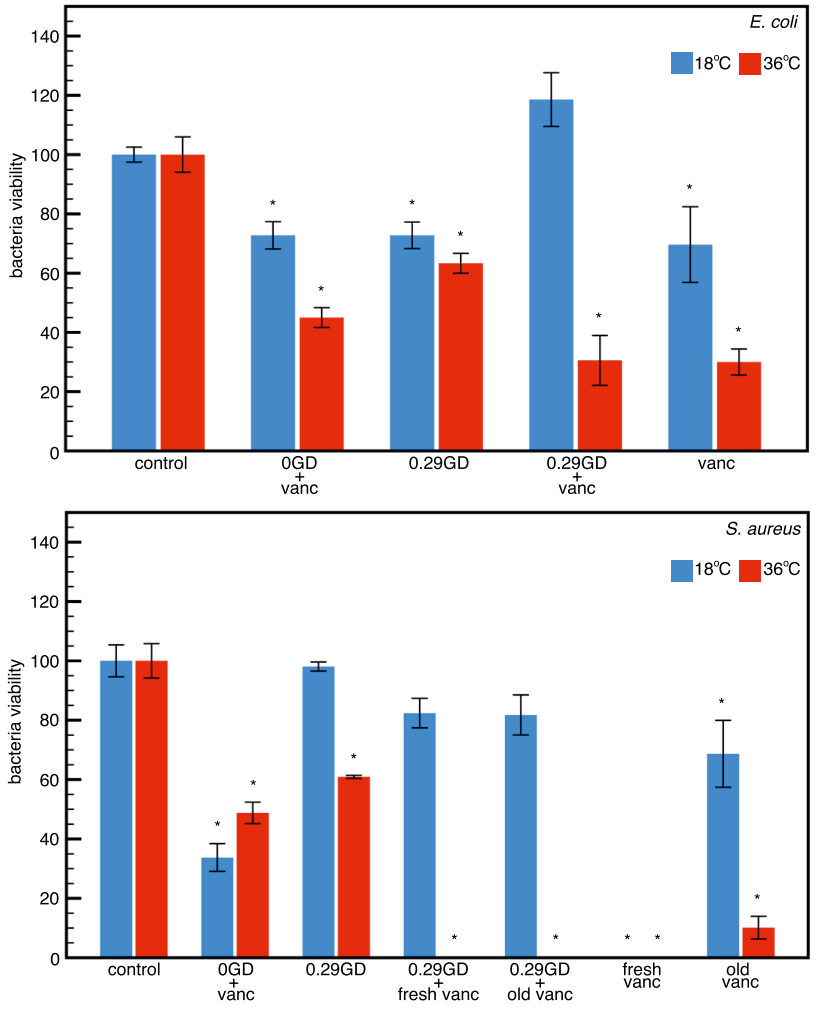

Figure 4. Normalized bacterial viability after exposure to PA particles with vancomycin adsorbed on the surface (0GD + vanc), PAPN (0.29GD), PAPN with encapsulated vancomycin (0.29GD + vanc), and vancomycin water solutions (vanc). *E. coli* bacteria were treated with samples stored for 2 weeks at room temperature, and *S. aureus* bacteria were treated with fresh and 1 month old samples. *E. coli* and *S. aureus* colonies were incubated with samples for 24 h at 18 and 36 °C. A statistically significant difference from the control was determined by a post hoc Tukey's HSD test and is denoted by a *. (*E. coli* 18 °C: n = 3, 3, 3, 3, 3; one-way analysis of variance (ANOVA), $F(4,10) = 24.005$, $p = 4.13 \times 10^{-4}$. *E. coli* 36 °C: n = 3, 3, 3, 3, 3; one-way ANOVA, $F(4,10) = 86.303$, $p = 1.04 \times 10^{-7}$. *S. aureus* 18 °C: n = 3, 3, 3, 2, 2, 3, 3; one-way ANOVA, $F(6,12) = 110.618$, $p = 8.52 \times 10^{-10}$. *S. aureus* 36 °C: n = 3, 3, 3, 3, 3, 3, 3; one-way ANOVA, $F(6,14) = 532.059$, $p = 1.08 \times 10^{-15}$).

cultures can be attributed to the bacteria−nanoparticle interactions resulting in a difference in the total number of bacterial colonies that could survive at each temperature. These results suggest that without an active shell, the PA nanoparticles will have a limited effectiveness and application. The PAPN system that was not loaded with vancomycin (0.29GD) showed a limited effectiveness suggesting that the nanocomposite by itself has minimal effect on both bacterial cultures. The PAPN system loaded with vancomycin (0.29GD + vanc) demonstrated the most significant effect on bacterial growth and the observed bacterial death can be attributed mostly to the vancomycin rather than the PAPN itself. In the *E. coli* bacterial cultures, the colonies held at a temperature below the LCST (18 °C) were able to maintain their viability; however, there was a significant decrease in the number of colonies as the temperature was increased above LCST (36 °C) due to the triggered release of vancomycin. The released vancomycin showed a comparable efficiency to that of the pure vancomycin. In the *S. aureus* bacterial cultures, the results were even more prominent. At a temperature below the LCST, only a small decrease in bacterial growth was observed for the PAPN system loaded with vancomycin (0.29GD + vanc), but at a temperature above the LCST, no living colonies were found on the Petri dish for all repetitions of the experiment. Another important observation was the difference in the activity of the fresh and old samples. Pure vancomycin cannot be stored for prolonged periods of time in water solutions,[10−13] and this can be clearly seen in results shown in Figure 4. After just 1 month, the solution of pure vancomycin (old vanc) had minimal effect on the *S. aureus* bacterial cultures at 18 °C, and even at 36 °C, some bacteria were able to survive. The vancomycin that was encapsulated in the PAPN system (0.29GD + fresh/old vanc) showed no decrease in activity after 1 month of storage in solution. This suggested that in addition to having a temperature-controlled release mechanism, the PAPN system can prolong the shelf life of the vancomycin solutions. This preservative effect would allow manufacturers to prepare solutions with exact concentrations in the controlled environment of a factory rather than leaving the preparation of the final solutions to pharmacy technicians.

It is important to note that pure vancomycin has a limited water solubility, while the PAPN system has much greater

https://dx.doi.org/10.1021/acs.langmuir.0c02385
Langmuir 2020, 36, 14607−14613

water compatibility due to the hydrophilic ethylene oxide (EO) chains of the poloxamer. The use of a carrier for the vancomycin that has an increased water compatibility allows the vancomycin to spread evenly throughout the solution volume. We suggest that the survival of some bacteria in the presence of pure vancomycin is due to degradation of vancomycin during storage.[12,13] As stated previously, *E. coli* was treated with 2 week old solutions and *S. aureus* was treated with fresh and 1 month old solutions. The observed results agree well with previously reported results for vancomycin-encapsulated polymer systems.[29]

The observed results demonstrate the benefits of drug encapsulation on antibacterial effectiveness over prolonged storage periods. The PAPN system proved to be effective in shielding the environment from the drug at temperatures below the LCST. Upon heating above the LCST, the PAPN system was able to release the preserved active form of the drug. This technology has the potential to be used for both bacterial diseases and cancer treatment due to its tunable, temperature-controlled release mechanism and its ability to deliver a high concentration of active molecules to a target region.

CONCLUSIONS

The bioavailability of the drug vancomycin can be improved through the use of a propargyl acrylate−poloxamer nanocomposite (PAPN) system. The temperature-stimulated, characteristic ability of a poloxamer to change the size and shape of its coils was exploited in this system to achieve a controlled release of the vancomycin. At temperatures below the lower critical solution temperature (LCST) of the poloxamer, the PAPN system was able to effectively encapsulate vancomycin such that the surrounding bacteria were unaffected and able to grow. At temperatures above the LCST of the poloxamer, the PAPN system was able to release the drug, which resulted in the death of the surrounding bacterial cells. Additionally, the PAPN system proved to be effective in protecting the encapsulated cargo from the environment until the temperature-triggered release. The vancomycin-encapsulated PAPN system offers a distinct advantage over the direct injection of free vancomycin molecules due to its ability for controlled release in target areas and its ability to preserve the drug activity.

AUTHOR INFORMATION

Corresponding Author

Stephen H. Foulger − *Department of Materials Science and Engineering, Center for Optical Materials Science and Engineering Technologies (COMSET), and Department of Bioengineering, Clemson University, Clemson, South Carolina 29634, United States;* orcid.org/0000-0002-4221-2154; Email: foulger@clemson.edu

Authors

Oleksandr Klep − *Department of Materials Science and Engineering and Center for Optical Materials Science and Engineering Technologies (COMSET), Clemson University, Clemson, South Carolina 29634, United States*

Haley W. Jones − *Department of Materials Science and Engineering and Center for Optical Materials Science and Engineering Technologies (COMSET), Clemson University, Clemson, South Carolina 29634, United States*

Vladimir Reukov − *Department of Textiles, Merchandising, and Interiors, University of Georgia, Athens, Georgia 30602, United States*

Complete contact information is available at: https://pubs.acs.org/10.1021/acs.langmuir.0c02385

Notes

The authors declare no competing financial interest.

ACKNOWLEDGMENTS

The authors thank the National Science Foundation (NSF) Grant # OIA-1632881 for financial support and Olga Reukova for help with the illustrations.

REFERENCES

(1) Radin, S.; Chen, T.; Ducheyne, P. The controlled release of drugs from emulsified, sol gel processed silica microspheres. *Biomaterials* **2009**, *30*, 2990−3006.

(2) Langer, R.; Peppas, N. A. Advances in biomaterials, drug delivery, and bionanotechnology. *AIChE J.* **2003**, *49*, 2990−3006.

(3) Kortesuo, P.; Ahola, M.; Kangas, M.; Leino, T.; Laakso, S.; Vuorilehto, L.; Yli-Urpo, A.; Kiesvaara, J.; Marvola, M. Alkyl-substituted silica gel as a carrier in the controlled release of dexmedetomidine. *J. Controlled Release* **2001**, *76*, 227−238.

(4) Rauschmann, M. A.; Wichelhaus, T. A.; Stirnal, V.; Dingeldein, E.; Zichner, L.; Schnettler, R.; Alt, V. Nanocrystalline hydroxyapatite and calcium sulphate as biodegradable composite carrier material for local delivery of antibiotics in bone infections. *Biomaterials* **2005**, *26*, 2677−2684.

(5) Radin, S.; Ducheyne, P. *Nanostructural Control of Implantable Xerogels for the Controlled Release of Biomolecules*; Springer: Dordrecht, 2004; Vol. *171*, pp 59−74.

(6) Radin, S.; Ducheyne, P.; Kamplain, T.; Tan, B. H. Silica sol-gel for the controlled release of antibiotics. I. Synthesis, characterization, and in vitro release. *J. Biomed. Mater. Res.* **2001**, *57*, 313−320.

(7) Anderson, K. E.; Eliot, L. A.; Stevenson, B. R.; Rogers, J. A. Formulation and evaluation of a folic acid receptor - Targeted oral vancomycin liposomal dosage form. *Pharm. Res.* **2001**, *18*, 316−322.

(8) Baral, A.; Roy, S.; Dehsorkhi, A.; Hamley, I. W.; Mohapatra, S.; Ghosh, S.; Banerjee, A. Assembly of an injectable noncytotoxic peptide-based hydrogelator for sustained release of drugs. *Langmuir* **2014**, *30*, 929−936.

(9) Ye, F.; Guo, H.; Zhang, H.; He, X. Polymeric micelle-templated synthesis of hydroxyapatite hollow nanoparticles for a drug delivery system. *Acta Biomater.* **2010**, *6*, 2212−2218.

(10) Sheldrick, G. M.; Jones, P. G.; Kennard, O.; Williams, D. H.; Smith, G. A. Structure of vancomycin and its complex with acetyl-n-alanyl-n alanine. *Nature* **1978**, *271*, 223−225.

(11) Ge, M.; Chen, Z.; Onishi, H. R.; Kohler, J.; Silver, L. L.; Kerns, R.; Fukuzawa, S.; Thompson, C.; Kahne, D. Vancomycin derivatives that inhibit peptidoglycan biosynthesis without binding d-Ala-d-Ala. *Science* **1999**, *284*, 507−511.

(12) Claudius, J.; Neau, S. The solution stability of vancomycin in the presence and absence of sodium carboxymethyl starch. *Int. J. Pharm.* **1998**, *168*, 41−48.

(13) Eff, A. R. Y.; Rahayu, S.; Tarigan, H. Stability and antibiotic activity vancomycin ophtalmic solution prepared from vancomycin dry injection against Pseudomonas eeroginosa and Staphylococcus aereus. *Int. J. Curr. Pharm. Res.* **2016**, *7*, 100−105.

(14) Bakhsheshi-Rad, H. R.; Hamzah, E.; Ismail, A. F.; Aziz, M.; Hadisi, Z.; Kashefian, M.; Najafinezhad, A. Novel nanostructured baghdadite-vancomycin scaffolds: In-vitro drug release, antibacterial activity and biocompatibility. *Mater. Lett.* **2017**, *209*, 369−372.

(15) Cevher, E.; Orhan, Z.; Mulazimoglu, L.; Sensoy, D.; Alper, M.; Yildiz, A.; Ozsoy, Y. Characterization of biodegradable chitosan microspheres containing vancomycin and treatment of experimental

osteomyelitis caused by methicillin-resistant Staphylococcus aureus with prepared microspheres. *Int. J. Pharm.* **2006**, *317*, 127−135.
(16) Kim, H. W.; Knowles, J. C.; Kim, H. E. Hydroxyapatite porous scaffold engineered with biological polymer hybrid coating for antibiotic vancomycin release. *J. Mater. Sci. Mater. Med.* **2005**, *16*, 189−195.
(17) Le Ray, A. M.; Chiffoleau, S.; Iooss, P.; Grimandi, G.; Gouyette, A.; Daculsi, G.; Merle, C. Vancomycin encapsulation in biodegradable poly(e-caprolactone) microparticles for bone implantation. Influence of the formulationprocess on size, drug loading, in vitro release and cytocompatibility. *Biomaterials* **2003**, *24*, 443−449.
(18) Burdette, M. K.; Jenkins, R.; Bandera, Y.; Powell, R. R.; Bruce, T. F.; Yang, X.; Wei, Y.; Foulger, S. H. Bovine serum albumin coated nanoparticles for in vitro activated fluorescence. *Nanoscale* **2016**, *8*, 20066−20073.
(19) Jenkins, R.; Bandera, Y. P.; Daniele, M. A.; Ledford, L. L.; Tietje, A.; Kelso, A. A.; Sehorn, M. G.; Wei, Y.; Chakrabarti, M.; Ray, S. K.; Foulger, S. H. Sequestering survivin to functionalized nanoparticles: A strategy to enhance apoptosis in cancer cells. *Biomater. Sci.* **2016**, *4*, 614−626.
(20) Daniele, M. A.; Bandera, Y. P.; Sharma, D.; Rungta, P.; Roeder, R.; Sehorn, M. G.; Foulger, S. H. Substrate-baited nanoparticles: A catch and release strategy for enzyme recognition and harvesting. *Small* **2012**, *8*, 2083−2090.
(21) Evanoff, D.; Hayes, S.; Ying, Y.; Shim, G.; Lawrence, J.; Carroll, J.; Roeder, R.; Houchins, J.; Huebner, C.; Foulger, S. Functionalization of crystalline colloidal arrays through click chemistry. *Adv. Mater.* **2007**, *19*, 3507−3512.
(22) Rungta, P.; Bandera, Y. P.; Tsyalkovsky, V.; Foulger, S. H. Designing fluoroprobes through Förster resonance energy transfer: Surface modification of nanoparticles through "click" chemistry. *Soft Matter* **2010**, *6*, 6083−6095.
(23) Alakhov, V.; Klinski, E.; Li, S. M.; Pietrzynski, G.; Venne, A.; Batrakova, E.; Bronitch, T.; Kabanov, A. Block copolymer-based formulation of doxorubicin. From cell screen to clinical trials. *Colloids Surf., B* **1999**, *16*, 113−134.
(24) Kabanov, A. V.; Batrakova, E. V.; Alakhov, V. Y. Pluronic block copolymers for overcoming drug resistance in cancer. *Adv. Drug Delivery Rev.* **2002**, *54*, 759−779.
(25) Alexandridis, P.; Hatton, T. A. Poly(ethylene oxide)-poly-(propylene oxide)-poly (ethylene oxide) block copolymer surfactants in aqueous solutions and at interfaces: Thermodynamics, structure, dynamics, and modeling. *Colloids Surf., A* **1995**, *96*, 1−46.
(26) Shubhra, Q. T. H.; Tóth, J.; Gyenis, J.; Feczkó, T. Poloxamers for surface modification of hydrophobic drug carriers and their effects on drug delivery. *Polym. Rev.* **2014**, *54*, 112−138.
(27) Alexandridis, P.; Holzwarth, J. F.; Hatton, T. A. Micellization of poly(ethylene oxide)-poly(propylene oxide)-poly(ethylene oxide) triblock copolymers in aqueous solutions: Thermodynamics of copolymer association. *Macromolecules* **1994**, *27*, 2414−2425.
(28) Batrakova, E. V.; Kabanov, A. V. Pluronic block copolymers: Evolution of drug delivery concept from inert nanocarriers to biological response modifiers. *J. Controlled Release* **2008**, *130*, 98−106.
(29) Censi, R.; Casadidio, C.; Dubbini, A.; Cortese, M.; Scuri, S.; Grappasonni, I.; Golob, S.; Vojnovic, D.; Sabbieti, M.; Agas, D.; Martino, P. Thermosensitive hybrid hydrogels for the controlled release of bioactive vancomycin in the treatment of orthopaedic implant infections. *Eur. J. Pharm. Biopharm.* **2019**, *142*, 322−333.

https://dx.doi.org/10.1021/acs.langmuir.0c02385
Langmuir 2020, 36, 14607−14613